TEMPORAL AND THERMAL PROPERTIES OF INTERMEDIATE-MASS FRAGMENTS FROM THE $^{32}S + ^{58}Ni$ REACTION AT 30 AMeV

A. TUTAY[1], A. BUDZANOWSKI[2], H. FUCHS[1], H. HOMEYER[1]

G. PAUSCH[3], C. SCHWARZ[4], A. SIWEK[2] AND A. TAYMAZ[5]

[1] Hahn-Meitner-Institut Berlin
Kernforschung Berlin Gmbh(HMI)
Glienicker Str.100, D-1000 Berlin 39, Germany
[2] Institute of Nuclear Physics
Radzikowskiego 152, 31-342 Cracow, Poland
[3] Forschungszentrum Rossendorf
Postfach 510119, D-01314 Dresden, Germany
[4] Gesellschaft für Schwere Ionen (GSI)
Postfach 110541, D-6100 Darmstadt 11, Germany
[5] University of Istanbul
TR-34459 Vezneciler, Istanbul, Turkey

(Received February 24, 1995)

Information on thermal and temporal aspects of intermediate-mass fragment (IMF) formation was obtained by studying correlations between (a) two IMFs, (b) one IMF and one α particle, and (c) one heavy residue and one α particle produced in collisions of 960 MeV ^{32}S projectiles with ^{58}Ni. The fragments and/or light particles were detected in the ARGUS multidetector array at the VICKSI accelerator of the HMI Berlin. The relative-energy distributions are of Maxwellian shape yielding a temperature of 5 MeV for the heavy reaction products, but only of about 3 MeV for the primary IMFs. Thus IMFs seem to be emitted towards the end of the evaporation chain. The relative-velocity correlations between two IMFs (Li, Be, B, C) display longer emission times when one of the IMFs is a lighter one (Li, Be), compatible with the picture that the latter are more likely to result from a multi-step decay.

PACS numbers: 25.70.Gh, 25.70.Mn, 25.70.Pq

1. Introduction

In the context of nuclear multifragmentation the question about the temperature of the primarily formed fragments arises. Multifragmentation

is understood to be the decomposition of a highly excited compound-nucleus (or incomplete-fusion product) into several — at least three — fragments of intermediate mass (IMFs). If this multifragmentation is due to critical fluctuations reflecting the nuclear analog of the ordinary liquid-gas phase transition (*cf.* the review of Gross [1]), the primary fragments should have a temperature close to the critical temperature of this transition, which by theoretical models is predicted to be at about 5 MeV or above [1]. In heavy-ion collisions at intermediate bombarding energies, fusion-like processes produce nuclei well inside the range of excitation energies where critical multifragmentation occurs. For instance in the system studied in this work, 30 AMeV ^{32}S + ^{58}Ni, complete fusion leads to 600 MeV excitation, the bulk of incomplete-fusion processes populates the range between 250 and 450 MeV [2], while the theoretical transition energy [1] is predicted to be at 330 MeV, corresponding to 4.3 MeV excitation energy per nucleon, or a temperature of 6.6 MeV. All this presumes a thermally equilibrated compound nucleus, while in practice, and in particular in heavy-ion collisions, a large part of the excitation energy may be stored in (non-thermal) collective modes. The latter possibly lead to decay modes quite different from that due to critical fluctuations, for example the often invoked "sequential fission", a sequence of temporally separated, independent binary splittings.

Apparently, also the mean time between the emission of two multifragmentation products (IMFs) is an interesting quantity possibly discriminating between sequential fission and the critical-fluctuation scenario connected with very short times ("simultaneous" fragment formation). Experimental information on this time may be obtained from relative-angle or from relative-velocity correlations [3]. In a previous study [2] we exploited relative-angle correlations, while in this work some results on relative-velocity correlations are given. At the same time, the temperature of primary IMFs is studied by measuring relative-energy distributions between α particles and the secondary IMFs, and the result is compared with the temperature of the compound nucleus derived from α particle evaporation spectra.

2. Experiment

The data analysed were taken in order to supplement the information from a previous experiment [2, 4] on the same system, 960 MeV ^{32}S + ^{58}Ni. A 1.0 mg/cm^2 thick ^{58}Ni target was irradiated for 44h with a ^{32}S beam of the average 1.4 nA electric current. The reaction fragments were recorded in the ARGUS multi-detector setup described previously [2]. It consisted of 108 detectors arranged on seven rings covering the angles from 3° to 41° with respect to the beam axis, and 20 further detectors on some selected angles further backward. The detectors were phoswich type scintillator combinations, except in five positions where they were replaced by

solid-state detectors serving as trigger detectors for the event registration. Different from the previous experiment [2, 4], these were two telescopes at $\Theta = 23.5°$ defining the reaction plane ($\phi = 0°$ and $180°$, respectively), one single solid-state detector at the same polar angle, but at $\phi = 45°$, and two such at $\Theta = 8°$ and $14°$ in the reaction plane.

A separate measurement was made with an 80 MeV ^{4}He beam on a carbon target yielding protons and α particles of discrete energies at forward angles used for the energy calibration of the phoswich detectors for these light particles. During the analysis of the solid-state detector data from the main experiment, a pulse shape effect was discovered enabling the discrimination of the fragment atomic number Z with a single detector in certain energy ranges [5]. This allowed in particular to determine the punch-through points of the various fragments up to $Z = 8$ providing calibration points for energy and time of flight. For the energy calibration of the phoswich detectors for fragments above $Z = 2$, we used the energy-light-output relation of Becchetti [6] with the values given for the exponents in the expression, and determined the factor describing amplification and light collection for the thin front scintillator from the punch-through point, for the thick E scintillator by matching the fragment spectrum with the spectrum in the solid-state detector at the same polar angle, the calibration of which does not depend on fragment Z (at least not below $Z = 10$). Taking the ratio of the amplification-collection factor between a given $Z > 2$ and $Z = 2$, we observed that this ratio is the same to within $\pm 10\%$ or better for all phoswich detectors of the same geometrical structure. So once a detector is calibrated for α particles, a calibration within this accuracy is directly provided for $Z > 2$ fragments.

3. IMF — α correlations

The question of primary IMF temperature was addressed by studying the example of excited primary oxygen fragments decaying into α particle and a carbon residue. Therefore coincidences between these two ejectiles were selected from the data. In order to provide information on the presumed parent oxygen nuclei, the ejectile momenta must be confined to domains where the sequential decay dominates over direct breakup modes (*cf.* Refs [7, 8]). According to systematics [8] this condition is generally fulfilled if the two decay products are detected at close-lying angles. Consequently we selected α particles in the phoswich detectors immediately adjacent to the trigger detector, the gate of which was set on carbon fragments. The trigger at the largest available angle, $\Theta = 23.5°$, was chosen because here one anticipates the largest contribution of IMFs originating from compound-nuclei or incomplete-fusion products. These are in the centre of interest.

The momenta or energies of the two coincident fragments were eventwise transformed into their common centre of mass (equal to the parent oxygen system), and each event was stored in bins of the relative α-carbon kinetic energy with a weight given by the Jacobian for the transformation.

Fig. 1 shows five such relative-energy distributions. They were evaluated for five subsequent intervals of the sum of kinetic energies of the two

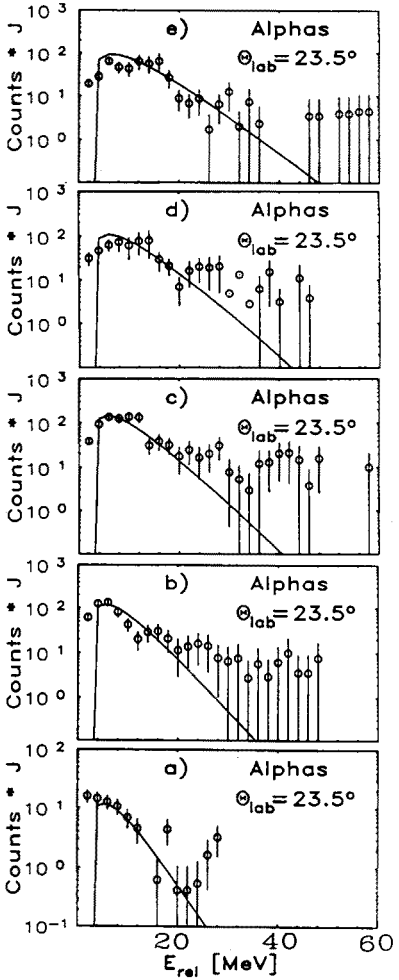

Fig. 1. Distribution of kinetic energy in the relative motion between coincident carbon fragments in the trigger at 23.5° and α particles detected in the adjacent phoswich detectors. Points: Experimental results after transformation into the emitter system. Curves: Maxwell fits (see text). Windows set on the sum of the laboratory kinetic energies of the two fragments are 50 to 100 MeV (a), 100 to 150 MeV (b), 150 to 200 MeV (c), 200 to 250 MeV (d) and all above 250 MeV (e).

particles, corresponding to increasing energy/velocity of the emitting excited oxygen nuclei. To the experimental spectra, Maxwell distributions of emission energy, const.$*(E_{\rm rel} - B)\exp[-E_{\rm rel}/T]$ were matched, where B is a barrier energy, and T the temperature and thus the interesting quantity. It is essentially determined by the exponential slope on the high-energy side of the spectrum. Some data points at the highest energies generally were omitted from the fitting procedure, as they are likely to represent some contribution of preequilibrium or direct α particle emission present at these angles to a certain degree.

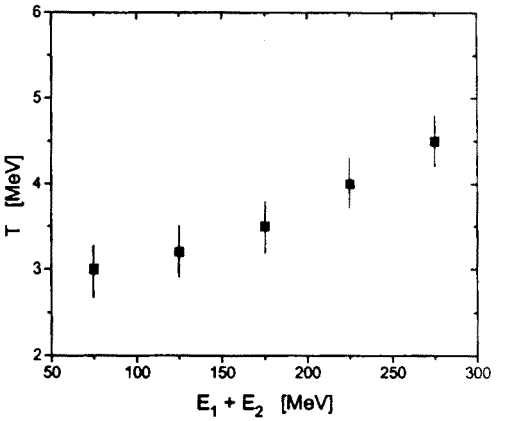

Fig. 2. Dependence of temperature parameter extracted from the spectra of Fig. 1 on the sum of fragment kinetic energies.

The extracted temperature values are displayed in Fig. 2 as a function of the sum energy. They apparently increase at higher emitter velocity. We attribute this to the fact that at higher emitter velocity, sequential emission and preequilibrium emission are less well separated in fragment velocity space, and the preequilibrium emission component is likely to influence the fit. Thus the higher apparent temperature in this range, $T > 4$ MeV, does not reflect a thermalized emitting system of such a temperature, but rather the influence of statistical properties of the preequilibrium emission. The present observation reminds of the argument made by Ref. [9] on the similar case of excited-state distributions in light-particle-IMF correlations: at emitter velocities close to the projectile velocity, the distribution width represents statistics of the Fermi motion set free by the direct breakup process, while at lower emitter velocities the additional excitation and equilibration of primary fragments entails more sequential decay processes enriching the low-temperature ranges finally observed. In any case, the temperature of 3 MeV approached when going to low emitter velocities represents the temperature of the decaying unstable oxygen fragments which are either due

to a deep-inelastic reaction or to emission from a highly excited compound nucleus or incomplete-fusion product.

4. Heavy residue — α correlation

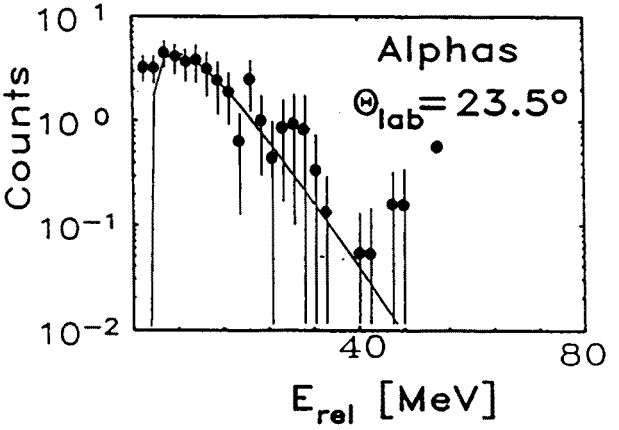

Fig. 3. Distribution of kinetic energy in the relative motion between coincident evaporation residues ($A > 40$) in the trigger detector at 23.5° and α particles detected at 48.5°. Points: experimental values after transformation into the emitter system. Curve: Maxwell distribution with $T = 5 MeV$.

It is interesting to compare with the temperature of compound-like nuclei. The latter has been extracted in very much the same way from the correlations between α particles detected at 48.5° and heavy residues recorded in the trigger detector at 23.5° . The relative-energy spectrum is shown in Fig. 3. The temperature extracted is 5 MeV, in agreement with previous results in the same system [2]. At the angle of 48.5° there is certainly little influence of preequilibrium emission. The clear difference between the two temperatures — 3 MeV and 5 MeV respectively — demonstrates that the oxygen fragments studied above clearly are emitted in a later phase of the deexcitation of the compound-like nucleus or intermediate complex. This result underlines the dominance of sequential emission already previously derived from the relative-angle correlations in IMF emission [2, 4].

5. IMF–IMF correlations

The question of the time scales ruling IMF emission is addressed by evaluating relative-energy correlations between two IMFs. Qualitatively, if

two IMFs are formed with a short time interval inbetween, the Coulomb repulsion between the two pushes them apart and thus depletes the distribution at small relative velocities or energies. In the correlation function, this shows up as a dip around 0 relative energy/velocity. With increasing time between the formation of the one and the other IMF, hence decreasing influence of the Coulomb repulsion, the dip gradually is filled in. The experimental correlation function is defined as

$$1 + R(v_{\mathrm{rel}}) = \frac{N_{\mathrm{cor}}(v_{\mathrm{rel}})}{N_{\mathrm{uncor}}(v_{\mathrm{rel}})}, \tag{1}$$

where N_{cor} is simply obtained by accumulating the coincidence events according to relative velocity v_{rel} between the two coincident fragments, while N_{uncor} is obtained from the same class of events by the event mixing procedure, *i.e.* by taking the measured energy of fragment 1 from one event, that of fragment 2 from the next event, and so on, and storing according to the relative velocity between these (clearly independent) fragments. Actually we evaluated the correlation function taking the so-called "reduced relative velocity" as variable,

$$v_{\mathrm{red}} = \frac{v_{\mathrm{rel}}}{(Z_1 + Z_2)^{1/2}}, \tag{2}$$

because in this variable the correlation functions for different $Z_1 + Z_2$ combinations, but the same mean emission time, should coincide to first order [11]. This facilitates the comparison between different distributions. The obtained IMF-IMF correlations, again for the triggering IMF at 23.5°, the other in the adjacent phoswich detectors, are displayed in Figs 4 and 5. Some of them clearly display the small-velocity dip reflecting the short-time Coulomb repulsion, others do not. The qualitative result immediately visible is that for pairs of carbon-carbon, boron-boron and carbon-boron the mean time elapsing between the formation of the two fragments is significantly shorter than for pairs with one or both fragments lighter than boron. Unfortunately the event rate was not sufficiently high to permit a subdivision of each distribution into separate distributions for several intervals of the summed kinetic energy as done with the data of Fig. 1. So it was not possible to judge the competing influence of projectile decay and emission from the heavy products of fusion-like processes. Both processes may contribute to the correlations shown which are based on all events with fragment energies above the experimental thresholds (typically 6 MeV/nucleon for carbon in the phoswich detectors). As the emitting source was not known, no model simulation of the correlation functions was attempted. Restricting to a qualitative discussion, for the sequential decay of for instance Mg* as a primary projectile-like fragment into two carbon nuclei one anticipates the short-time emission pattern observed, as the two fragments

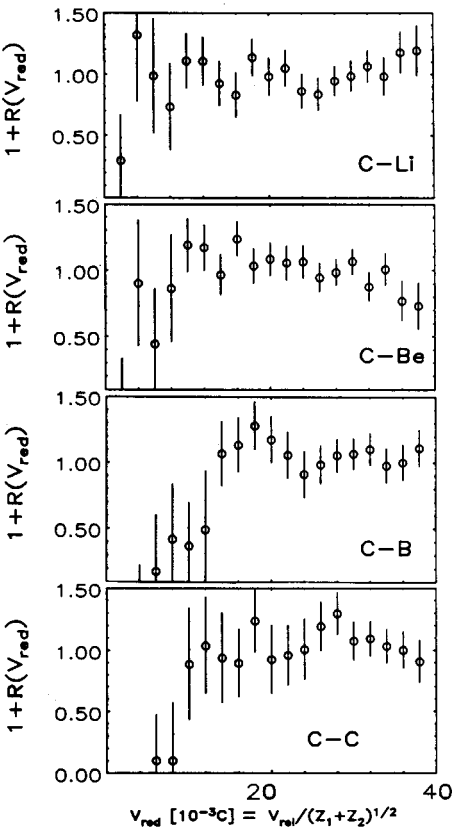

Fig. 4. Experimental relative-velocity correlation functions according to Eq. (1) between coincident carbon fragments in the trigger at 23.5° and IMFs ($Z = 3$ to 6) in phoswich detectors at 14°, 18.5° and 23.5°. The abscissa is the reduced relative velocity (see text).

are trivially formed in the very same moment of time. The situation is very similar in case of the direct production of two fragments which probably dominates at the bombarding energy chosen [10]. For emitted α particles we know that sequential emission makes a sizable contribution to the cross-section [7]. Thus we may conclude that the lighter the fragment, the higher is the probability that it was emitted as a result of a sequential decay. This may explain to some extent the trend toward longer times for light fragment emission seen in the correlation functions.

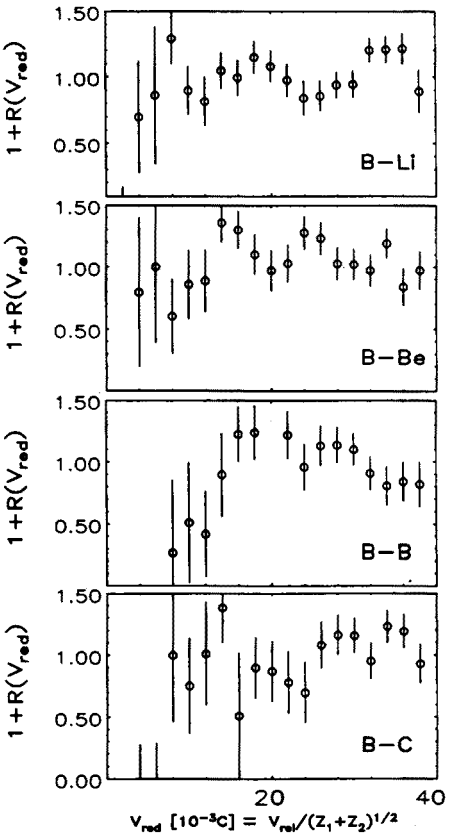

Fig. 5. Same as Fig. 4, but with boron fragments in the trigger detector.

6. Conclusions

As for the behaviour of IMF emission by heavy excited products of fusion-like reactions, we know from the relative-angle correlations [2] that sequential emission dominates, with a possible contribution of simultaneous formation of at most 30%. This result was derived globally for all IMFs ($Z > 2$), without further specification of fragment Z. In principle it would be possible that in the present investigation, by selecting pairs of carbon or boron fragments, one happens to hit precisely the possibly present simultaneous-decay component of multifragmentation. This argument stays, however, hypothetical in view of the certainly contributing projectile decay.

To conclude, the IMF-IMF relative-velocity correlations display a qualitative dependence of mean emission time on fragment mass, which is compatible with the dominance of sequential IMF emission from highly excited

products of fusion-like processes. On the other hand, the temperatures extracted from α particle emission spectra provide an independent confirmation of the indicated sequential IMF formation picture.

REFERENCES

[1] D.H.E. Gross, *Rep. Progr. Phys.* **53**, 605 (1990).

[2] A. Siwek, A. Sourell, A. Budzanowski, H. Fuchs, H. Homeyer, G. Pausch, W. Kantor, G. Röschert, C. Schwarz, W. Terlau, A. Tutay, *Z. Phys.* **A350**, 327 (1995).

[3] J.A. Lopez, J. Randrup, *Nucl. Phys.* **A491**, 477 (1989).

[4] A. Siwek, A. Budzanowski, H. Fuchs, H. Homeyer, W. Kantor, G. Pausch, G. Röschert, C. Schwarz, A. Sourell, W. Terlau, A. Tutay, *Acta Phys. Pol.* **B25**, 765 (1994).

[5] G. Pausch, W. Bohne, H. Fuchs, D. Hilscher, H. Homeyer, H. Morgenstern, A. Tutay, W. Wagner, *Nucl. Instr. Methods Phys. Res.* **A322**, 43 (1992); G. Pausch, W. Bohne, D. Hilscher, H.-G. Ortlepp, D. Polster, *Nucl. Instr. Methods Phys. Res.* **A349**, 281 (1994).

[6] F.D. Becchetti, C.E. Thorn, M.J. Levine, *Nucl. Instr. Methods Phys. Res.* **138**, 93 (1976).

[7] C. Schwarz, H. Fuchs, H. Homeyer, K. Möhring, T. Schmidt, A. Siwek, A. Sourell, W. Terlau, A. Budzanowski, *Phys. Lett.* **B279**, 223 (1992).

[8] H. Fuchs, K. Möhring, *Rep. Progr. Phys.* **57**, 231 (1994).

[9] H. Fuchs, H. Homeyer, *CORINNE 90 Nantes*, ed. D. Ardouin, World Scientific, Singapore 1990, p.305.

[10] C. Schwarz, H. Fuchs, H. Homeyer, K. Möhring, T. Schmidt, A. Siwek, A. Sourell, W. Terlau, A. Budzanowski, *Z. Phys.* **A345**, 29 (1993).

[11] Y.D. Kim, R.T. de Souza, D.R. Bowman, N. Carlin, C.K. Gelbke, W.G. Gong, W.G. Lynch, L. Phair, M.B. Tsang, F. Zhu, *Phys. Rev.* **C45**, 387 (1992).